Environ Geol (2006) 50: 147–155
DOI 10.1007/s00254-006-0194-4

ORIGINAL ARTICLE

Mahmut G. Drahor
Gökhan Göktürkler
Meriç A. Berge
T. Özgür Kurtulmuş

Application of electrical resistivity tomography technique for investigation of landslides: a case from Turkey

Received: 12 December 2005
Accepted: 4 February 2006
Published online: 25 February 2006

M. G. Drahor (✉) · T. Özgür Kurtulmuş
Center for Near Surface Geophysics and Archaeological Prospection (CNSGAP), Dokuz Eylül University, Tınaztepe Campus, 35160 Buca, İzmir, Turkey
E-mail: goktug.drahor@deu.edu.tr
Tel.: +90-232-4127221
Fax: +90-232-4538366

M. G. Drahor · G. Göktürkler
M. A. Berge
Engineering Faculty, Department of Geophysics, Dokuz Eylül University, Tınaztepe Campus, 35160 Buca, İzmir, Turkey

Abstract Electrical resistivity imaging is a widely used tool in near surface geophysical surveys for investigation of various geological, environmental and engineering problems including landslide. In this study, an electrical resistivity tomography (ERT) survey was conducted in a landslide area, located in the Söke district of Aydın, Turkey. In 2003, the Neogene-aged units on the slope next to a newly built school building became unstable due to an excavation work and moved after a heavy rainfall. The resulting landslide partly covered the school. The authors carried out a 2-D resistivity survey along three profiles over the landslide mass using a Wenner configuration. It yielded useful information about the geometry and characteristics of the landslide. In addition, a 2-D synthetic resistivity modelling study was carried out to understand the response of the resistivity method to a landslide problem before the field surveys. Eight boreholes were also drilled in the landslide area. Both the drilling and resistivity results indicated the presence of a fault in the site. Also, the resistivity data from the line measured along the axis of the landslide revealed the surface of rupture.

Keywords Electrical resistivity tomography · Landslide · Söke · Turkey

Introduction

Surface geophysical methods have been performed in the investigation of slope stability for 35 years. Owing to rough topographical changes in landslide areas, it is difficult to conduct such surveys. Recently, some geophysical imaging techniques based on the tomographic inversion have been routinely used in shallow investigations as a result of the advancements in computer technology and numerical methods. Thus, the electrical resistivity tomography (ERT) and seismic imaging methods have been widely employed in landslide surveys (Batayneh and Al-Diabat 2002; Bichler et al. 2004; Konagai et al. 2005).

Electrical surveys may be a useful tool for the fast investigation of the geometry, water content and fluid movement of subsurface. The resistivity method is one of the standard methods of the geophysical prospecting for solution of shallow geological problems. It is also useful to determine some characteristics of landslides such as main body, geometry, surface of rupture and it has been used in landslide investigations since late 1970s (Bogoslovsky and Ogilvy 1977; Caris and Van Ash 1991; Hack 2000; Havenith et al. 2000; Yang et al. 2004). Originally, it was performed as the vertical electrical sounding (VES) in landslide investigations. Today, a 2- or 3-D resistivity measurement is a common application of the method in slope stability investigations (Suzuki and Higashi 2001; Lapenna et al. 2003).

After a heavy rainfall, a landslide occurred in the Söke district of Aydın located in the Aegean Region of Turkey in 2003. This instability partly damaged a newly built

elementary school building. Some geotechnical and drilling studies were performed after the landslide (E.T. Sondaj, unpublished data). However, the drilling results were not sufficient to determine landslide geometry. Therefore, a 2-D resistivity survey was carried out along three lines using a Wenner electrode configuration. One of the lines was along the axis of the landslide, whereas the others were across the landslide mass. The data were processed by a resistivity inversion technique to achieve electrical imaging along these lines. The ERT study was helpful for defining the geometry and some physical properties of the landslide mass. A good match between the resistivity and drilling results was also observed. Thus, this paper aims to discuss the results of these studies.

Site characteristics

Geological setting

The landslide area is situated on the Neogene-aged Söke formation in the town of Söke, western Anatolia (Fig. 1a, b). This formation crops out in northern and northwestern part of the Büyük Menderes graben, which is one of the major E–W trending grabens of western Anatolia (Yılmaz et al. 1999; Seyitoğlu and Scott 1992; Sarıca 2000). The N–S trending Neogene-Quaternary deposits are observed between the towns of Söke and Kuşadası. This sequence is delimited by the fault of the Büyük Menderes graben and the Aegean Sea. The faults that encircled this sequence are active, and the last big earthquake ($M = 6.8$) occurred on the Söke-Balat fault system in 1955 (McKenzie 1972). The Söke Neogene basin is bounded by steeply dipping normal faults towards the town of Kuşadası (Fig. 1b).

According to Gürer et al. (2001), the general stratigraphy of this area is represented by three major rock groups. The metamorphic rocks of the Menderes Massif form the basement, which is overlain by the Neogene sedimentary rocks. The second major group, which covers the Menderes Massif, is originated by Miocene-aged units (Kemalpaşa conglomerate, Söke formation, Maden limestone, Davutlar conglomerate, Fevzipaşa and Kuşadası formation and Hisartepe volcanics) (Figs. 1c, 2). The uppermost sequence comprises the Yamaçköy conglomerate and sandstone of Neogene and the Quaternary alluvium (Figs. 1c, 2). The Neogene units were extremely deformed by folding and faulting mechanism after the Late Miocene–Early Pliocene. The general folding trends are in the directions of ENE–WSW and NNW–SSE, while the faults extend in the directions of E–W, NE–SW and NNW–SSE (Yılmaz et al. 1999; Gürer et al. 2001) (Fig. 1b, c).

The study area is located in the northwestern part of the Söke town (Fig. 1b, c). The mica schist consisting of the chlorite, muscovite and quartzites are observed in the southern part of the investigated area, and belongs to the Menderes Massif. It is covered by the Söke formation with an angular unconformity in the northern part of the investigation area, and it comprises sandstone, siltstone and mudstone, also includes thinly bedded lignite. In addition, some old landslides are evident in topographic maps and by field observations (Figs. 3, 4). There is a newly built elementary school building in the northeastern part of the area. Some excavations were carried out for the construction of a second garden in the south of the school building in 2003. Owing to these excavations, the weak Neogene units forming the slope of the hill adjacent to the school building moved after a heavy rainfall, and the resulting landslide damaged the school. Some parts of the ground and first floors of the building were occupied by the landslide materials (Fig. 4a, b). This prevented the school from public use for about 3 years. Figure 4c illustrates the main features of the resulting landslide (main and minor scarps and head), and the resistivity line along the direction of landslide movement is also shown on the figure.

Borehole data

Some drilling work related with the geotechnical investigations was immediately performed after the landslide. Eight boreholes were drilled over the landslide materials and its neighbourhood (Fig. 3) (E.T. Sondaj, unpublished data). The depth range of the boreholes varies between 15 and 30 m, and the total depth was about 166 m. Figure 5 demonstrates the whole borehole data together with the groundwater levels. Each well is depicted on the figure with respect to their elevations. According to this, the thickness of the landslide material changes from 3.5 to 10 m. Table 1 also gives a list of borehole data.

The boreholes SK-5 and SK-6 were located in high elevations of the study area. The logs of these boreholes demonstrate results similar to each other. The landslide material was about 10 m thick and sandstone was cut until the bottom of the boreholes. They have groundwater level at 7.5 m. The boreholes SK-3 and SK-4 were drilled near the second head of the landslide. The depths of the boreholes SK-3 and SK-4 were 30 and 20 m, respectively. The groundwater level was at 8 m in SK-3 and 7.5 m in SK-4. The landslide material was observed till 9 m in SK-3 and 8 m in SK-4. Then, clay, mud and sand were penetrated down to 21 m in borehole SK-3. They were followed by thickly bedded, grey-beige sandstone until the bottom of the hole. However, the landslide material was directly underlaid by the thickly bedded sandstone till the bottom of SK-4 (Fig. 5, Table 1).

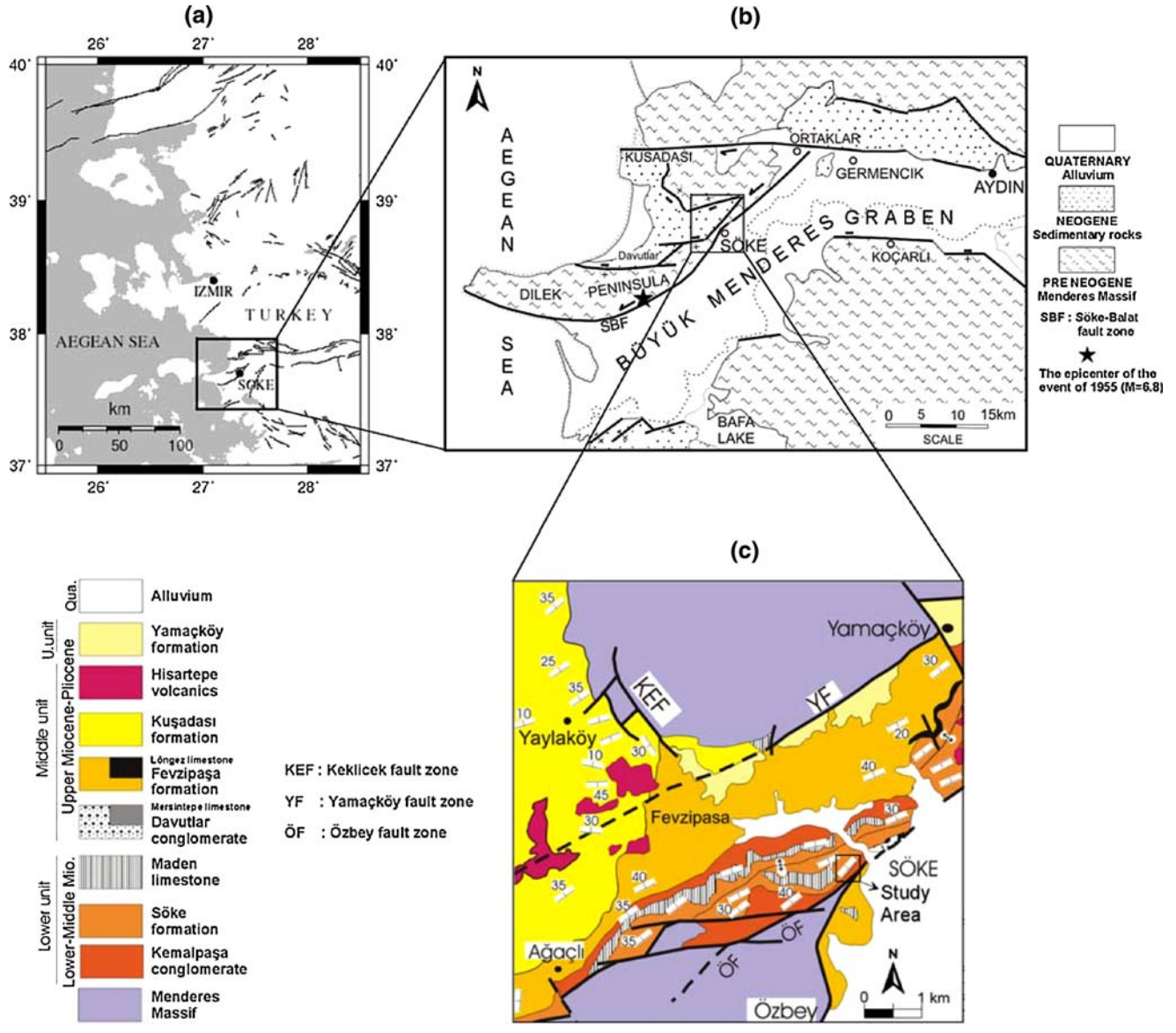

Fig. 1 **a** Location of the study area with the active faults of western Anatolia, **b** geological map of Söke and its surrounding (after Gürer et al. 2001), **c** detailed geological map of the study area and its surrounding (after Gürer et al. 2001)

The boreholes SK-1 and SK-2 were drilled near the toe of the landslide, and the distance between them was 16 m. These boreholes were 20 m deep, and the groundwater level was observed at 3.5 m in both of them. Lithological logs show that the landslide material is highly mixed in these wells. The disturbed material due to the landslide continues until 6 and 4.5 m in SK-1 and SK-2, respectively. Then, the sandstone, which is grey-beige in colour, thinly bedded and includes a lignite layer, was encountered in these boreholes. This unit is considered as the Söke formation (Fig. 5, Table 1).

SK-7 and SK-8 were situated in the southeastern part of the investigation area. SK-7 was 18 m deep, and groundwater level was at the surface. Three geologic units were identified in this borehole. The first layer extends from the surface to the depth of 3 m and includes clay and sand. The second one is composed of rounded pebbles only, while the last one is the schist of the Menderes massif and is observed till the bottom of the borehole. SK-8 borehole was 15 m deep, and groundwater level was at the depth of 1.5 m. Clay, mud and sand were firstly observed at the depth of 3 m in this borehole. Then, the schist of the Menderes Massif was cut until the bottom of the hole. The landslide material was absent in these boreholes. These two boreholes give different results than the others. The authors consider

that a fault between the boreholes SK-2 and SK-7 might be responsible for this (Fig. 5, Table 1).

As a result, the borehole data were not satisfactory for defining the landslide geometry and also raised the question of a fault. Thus, an electrical resistivity imaging survey was carried out to investigate the landslide and the existence of a fault.

Resistivity studies

2-D electrical resistivity tomography survey

A resistivity survey aims to determine the resistivity distribution in the subsurface by making measurements along the ground surface. It is based on measuring the electrical potential between a pair of electrodes caused by direct current injection between another pair of electrodes. Then the apparent resistivity is measured. Data are generally presented in the form of a pseudo-section, which is a representation of the apparent resistivity variations in the subsurface.

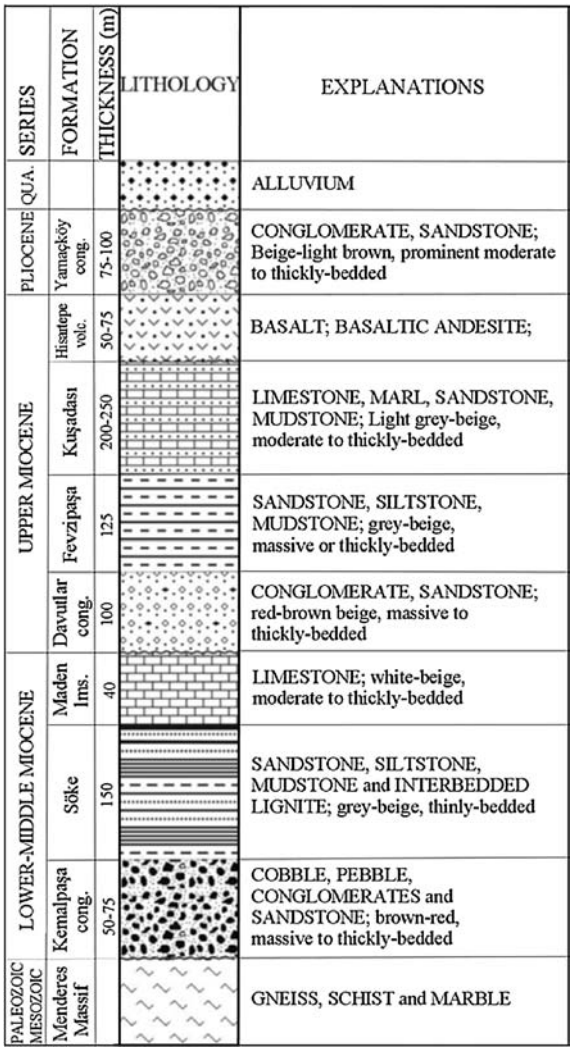

Fig. 2 Generalized stratigraphic section of the Söke-Kuşadası region (after Gürer et al. 2001)

Two-dimensional electrical resistivity tomography studies are generally performed by using a multi-electrode cable. The arrangement of electrodes for different configurations is managed by a resistivitymeter that has an electronic switching unit and a personal computer (Griffiths and Barker 1993). Today, resistivity equipments and data acquisition techniques for 2- and 3-D surveys advance very fast. Thus, many engineering and shallow geological problems may be quickly investigated in detail by using multi-electrode resistivitymeters.

The resistivity survey in the study area was conducted along three lines. Line-1 and -2 were across the landslide mass while Line-3 was along the landslide axis (Fig. 3). Data were acquired by a Wenner configuration using a 30-electrode cable 5 m apart. A 2-D tomographic inversion technique was employed to process the data using RES2DINV software. The method is based on the smoothness-constrained least-squares inversion of pseudo-section data (Tripp et al. 1984; deGroot-Hedlin and Constable 1990; Sasaki 1992; Loke and Barker 1996). In this algorithm, the subsurface is divided into rectangular blocks of constant resistivity. Then the resistivity of each block is evaluated by minimizing the difference between observed and calculated pseudo-sections using an iterative scheme. The smoothness-constraint leads the algorithm to yield a solution with smooth resistivity changes. The calculated pseudo-sections can be obtained by either finite-difference or finite-element methods (Coggon 1971; Dey and Morrison 1979). In this case, the finite-element scheme was employed due to the topographical changes in the field.

Synthetic resistivity modelling study for the rotational landslide

The synthetic modelling studies mostly help to understand the response of the resistivity method to different geological and engineering problems before the field surveys. Therefore, the authors firstly performed a 2-D synthetic resistivity modelling study considering a rotational landslide, which is a common type of mass movement. It has upward concavely curved surface of rupture, and the slide material makes a rotation about the axis, which is parallel to the ground surface and across the landslide (USGS 2004). In addition, based on the geologic observations and borehole results in the study area (Fig. 3), a lateral discontinuity between the resistivity zones of 10 and 35 Ωm was also included into the model. Since the groundwater level was very close to the surface, the authors assigned relatively low resistiv-

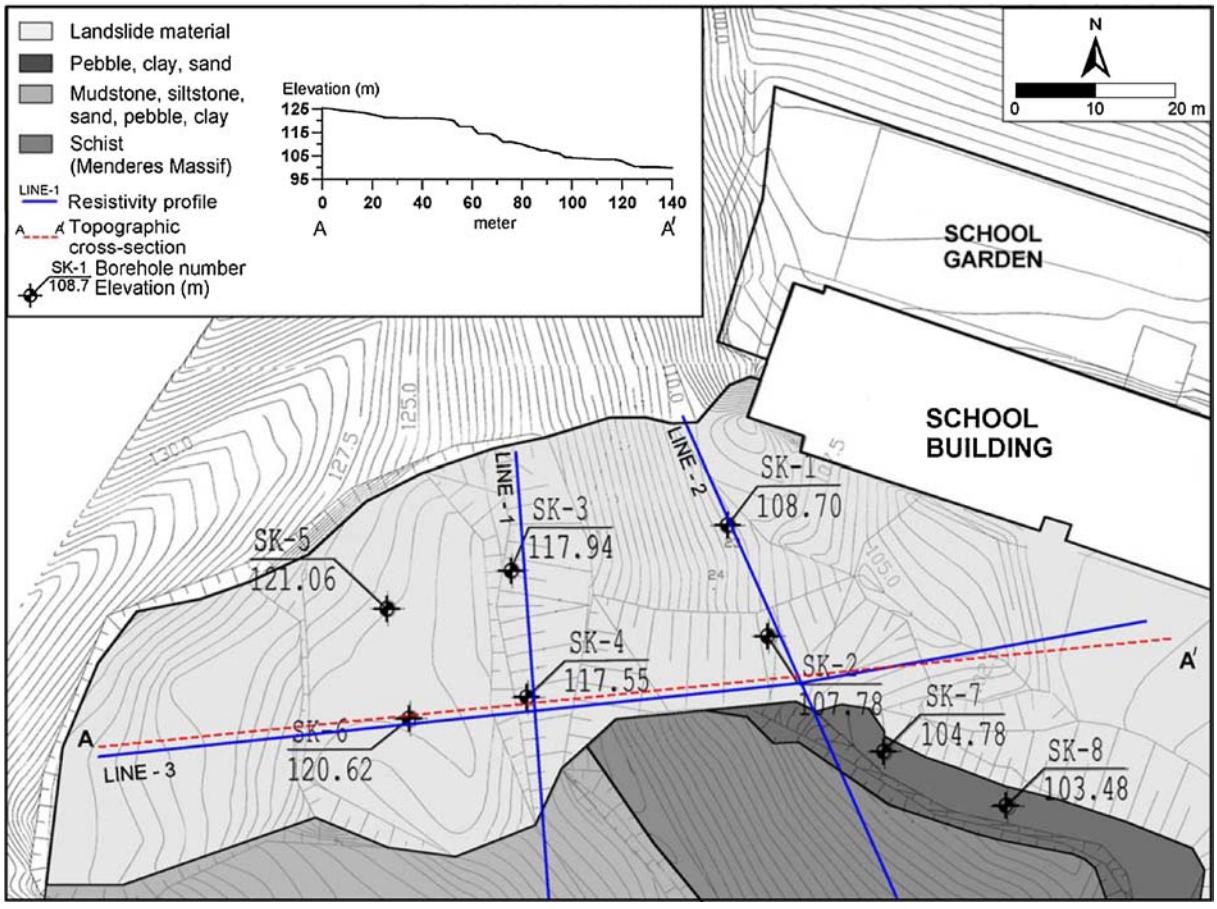

Fig. 3 Geological and topographical map of the Söke landslide area. Resistivity lines and borehole locations are also depicted on the figure. The inset shows topographical cross-section (A–A′) along the landslide movement (modified from E.T. Sondaj, unpublished data)

ities to the units in the model considering the possibility of high water content of the geologic units in the field. Figure 6a shows this model together with the assigned resistivity values. The geologic units and assigned resistivities are also given in Table 2. The modelling was achieved in two steps. In the first step, a pseudo-section was calculated for a Wenner electrode configuration using RES2DMOD software (Geotomo software 2005a). Figure 6b displays the resulting pseudo-section. The effects of the geologic units about the discontinuity between the distances of 70 and 90 m are observed. Then this pseudo-section was inverted by RES2DINV software (Geotomo software 2005b) to reconstruct the resistivity distribution in the model. The smoothness-constrained least-squares scheme was used to achieve this step. At the end of five iterations, the resistivity section shown in Fig. 6c was obtained with an RMS error of 1.2%. One can easily observe that the resistivity section reveals main features of the model in Fig. 6a. The resistivity values evaluated are also very close to the original ones.

Results

The resistivity survey was performed right after a heavy rain. Thus, the slope-forming material was saturated. Obviously, this condition affected the resistivities in the subsurface and a data set displaying relatively lower apparent resistivities was obtained. Figure 7 shows the results of electrical resistivity tomography. The simplified logs of the boreholes are also depicted on the resulting tomograms. The data along Lines-1 and -2 were measured in perpendicular directions to the landslide movement. Line-1 was approximately in the direction of N–S (Fig. 3). The length of the line was about 60 m, and the measuring surface was rather flat. The resulting tomogram along this profile suggests relatively low resistivity values. They are in the range of 20–40 Ωm, and there are two distinct resistivity zones along the line. High resistivities are generally obtained in the northern and southern parts of the line. They relatively increase with depth in the southern part of the line. The zone of low

Fig. 4 **a**, **b** Views from the study area after the landslide, **c** the main features of the landslide together with the resistivity profile Line-3

resistivity (10–20 Ωm), located in the middle part of the section, probably represents the landslide materials with higher water content. There are two boreholes (SK-3 and SK-4) on Line 1. Landslide material, clay, mud and sand units observed in these boreholes are in good agreement with the results of the electrical resistivity tomography. The resistivity values relatively increase with depth in the sandstone unit (Fig. 7a).

Line-2, which is nearly perpendicular to the direction of landslide movement, runs from NW to SE (Fig. 3). It is 60 m in length, and has almost flat lying surface. As can be seen from Fig. 7b, the resistivity distribution in Line-2 differs from that in Line-1. The resistivities are very low (9–20 Ωm) in the northwestern part of the line (between 35 and 60 m), while they are rather high (20 and 115 Ωm) in the southeastern part of the line (between 0 and 35 m). In addition, the resistivities suddenly change in the middle of the line. The low resistivity might be caused by the water content of the unconsolidated material while the higher values might be an indicator of the consolidated materials. Thus, it can be concluded that there might be a fault at this location. There are three boreholes (SK-1, SK-2 and SK-7) on this line. The electrical tomography image is in good agreement with the results of boreholes. The borehole SK-7 displays very different results than SK-1 and SK-2. Also, this situation is clearly observed in the electrical resistivity tomogram (Fig. 7b). The schist unit in SK-7 is characterized by high resistivity values on the tomogram, while the clay, mud, sand and pebbles have moderate resistivities. Thus, the presence of a fault, suggested by the borehole data, is clearly verified by the resistivity results (Fig. 7b).

The third line (Line-3) was along the direction of the landslide movement. The line is about 130 m long, and it is in the direction of ENE–WSW (Figs. 3, 4). The ERT result obtained along this line is shown in Fig. 7c. The resistivity section along this line demonstrates very informative result in determination of the geometry of the landslide. It clearly reveals the subsurface geometry of the landslide. It is considered that the layer with relatively high resistivity (15–35 Ωm) observed in shallow depths might be originated by the landslide material. The thickness of this layer varies between 3 and 5 m on the tomogram. Also, one can observe that this zone is related with the topographical changes and the depth of groundwater level. Then, a conductive zone, which has a resistivity ranging from 5 to 15 Ωm, is observed, and its thickness varies between 5 and 15 m. This zone seems very similar to rotational landslide type. But, this is not supported by borehole data because there is no borehole penetrating into this zone. This conductive layer might be composed of unconsolidated and water-saturated landslide material that contains clay, mud, sand and silt. The water content is considered for low resistivities, and this might be the key parameter in sliding. Thus, the bottom of this zone can be the failure surface of the recent landslide. The zone of relatively high resistivity (28–52 Ωm) between the horizontal distances of 75–110 m resembles the toe of the surface of rupture. It might be formed by the consolidated units of the Menderes Massif (probably schist). Furthermore, the resistivity tomography image shows that the geometry of the landslide is in the rotational form, and it demonstrates features similar with the result of the previous synthetic modelling study (see Fig. 6c). The electrical tomography section crosses the locations of three boreholes (SK-2,

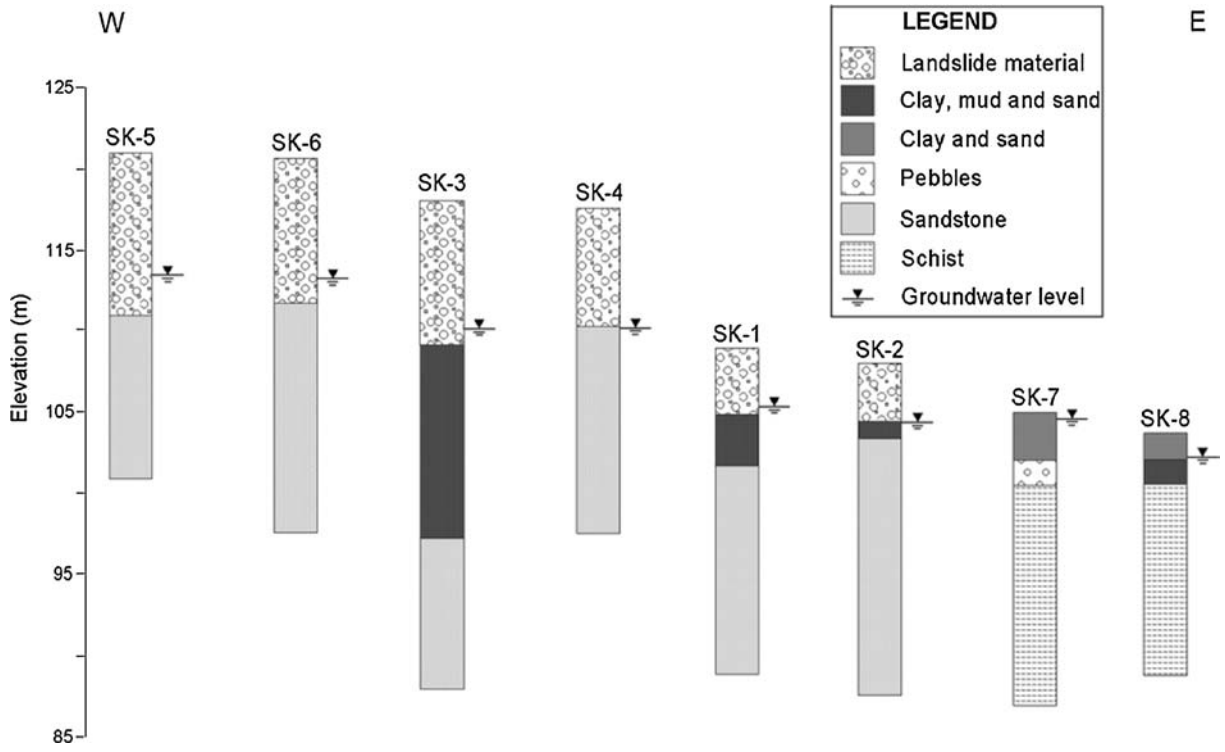

Fig. 5 Simplified lithological logs of boreholes drilled in the landslide area (modified from E.T. Sondaj, unpublished data)

Table 1 Borehole data

Boreholes	Drill depth (m)	Groundwater level (m)	Lithological unit
SK-1	20	3.5	Landslide material, clay, mud, sand and sandstone
SK-2	20	3.5	Landslide material, clay, mud, sand and sandstone
SK-3	30	8.0	Landslide material, clay, mud, sand and sandstone
SK-4	20	7.5	Landslide material, sandstone
SK-5	20	7.5	Landslide material, sandstone
SK-6	23	7.5	Landslide material, sandstone
SK-7	18	3.5	Clay, sand, pebbles and schist
SK-8	15	1.5	Clay, sand, mud and schist

Table 2 Lithological unit and assigned resistivities for synthetic landslide model

Geologic unit	Resistivity (Ωm)
Schist (saturated)	35
Sandstone, siltstone, mudstone (grei-beige, thinly-bedded)	25
Sandstone, siltstone, mudstone (grei-beige, massive or thickly-bedded)	10
Landslide materials	60

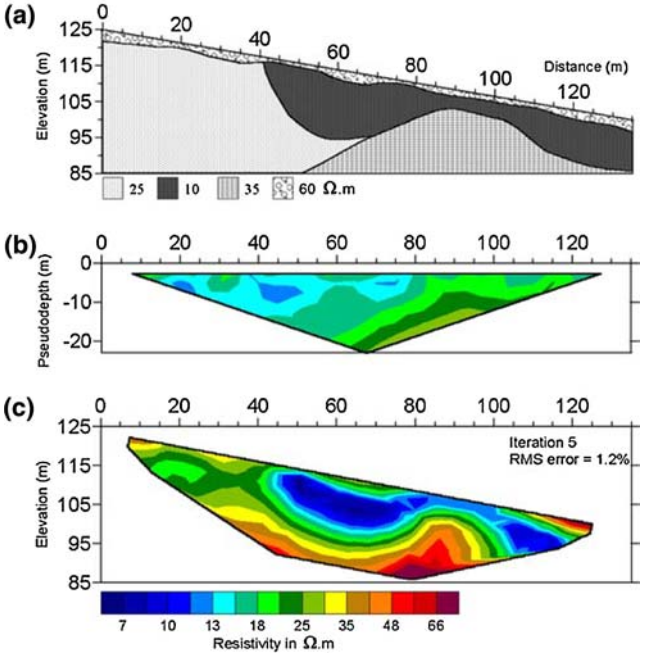

Fig. 6 Resistivity modelling of a landslide model: **a** the conceptual model, **b** the apparent resistivity pseudo-section for a Wenner configuration **c** the resistivity tomogram obtained by inversion method.

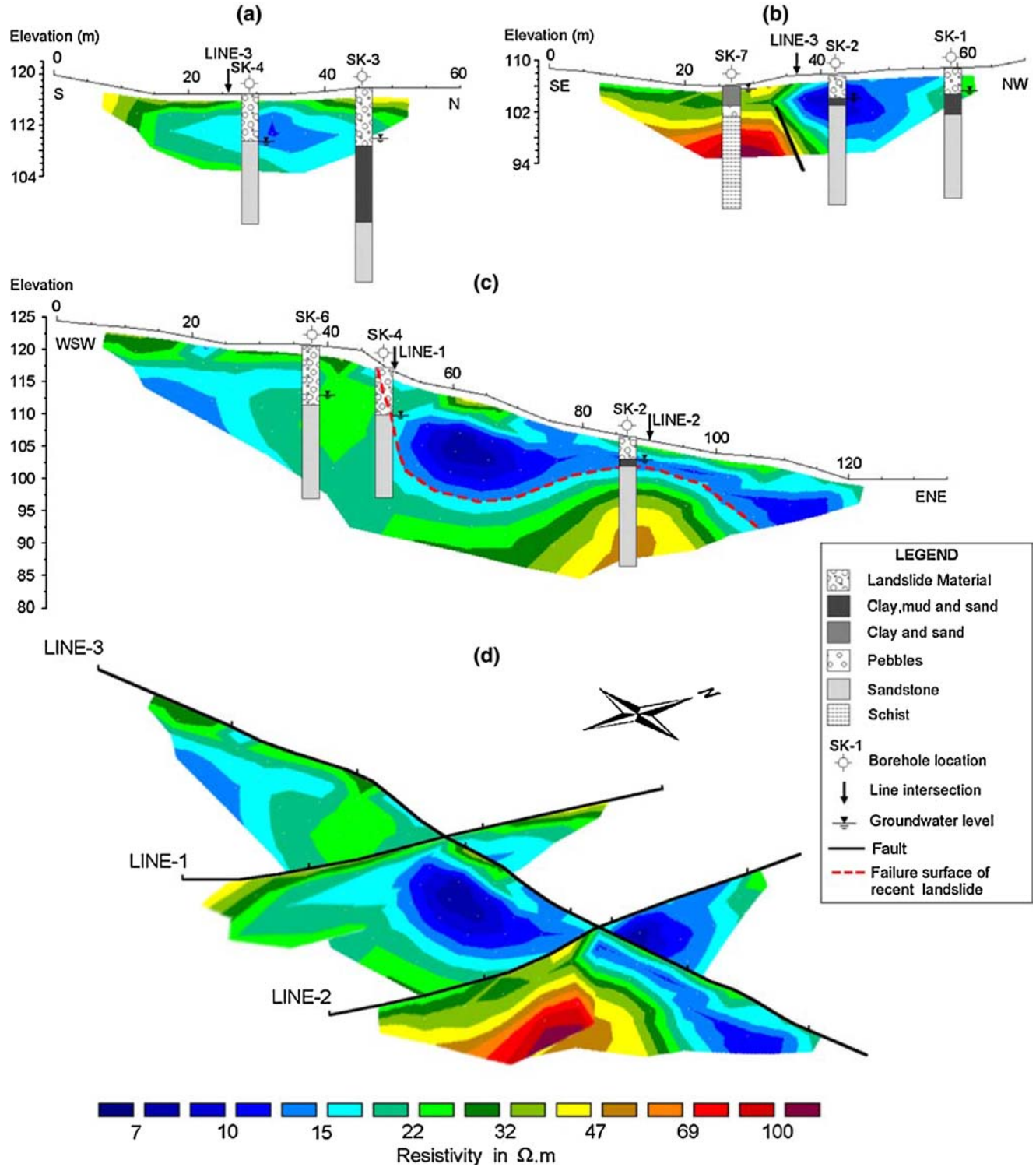

Fig. 7 Electrical resistivity tomography results: **a** Line-1 and **b** Line-2 along the perpendicular direction to the landslide movement, **c** Line-3 obtained along the direction of landslide movement (for location, see Fig. 3), and **d** 3-D fence diagram of the resistivity sections

SK-4 and SK-6), and the resistivity results were confirmed by the borehole data (Fig. 7c). Figure 7d illustrates the ERT results in the form of a 3-D fence diagram. There is a good match among the resistivity sections. It also displays the presence of a fault and its relation with the landslide body.

Conclusions

In this study, a landslide case from Turkey is presented. In 2003, a landslide occurred in the Söke district of Aydın, and damaged a school building by occupying its some parts. This caused a 3-year delay in education in the school. This case study shows that the electrical resistivity tomography is a useful tool for the investigation of landslides. The geometry and some physical properties of the landslide material as well as water-saturated zones might be determined by the resistivity imaging. Performing a synthetic modelling before the field investigation can also be useful in a landslide survey.

In this study, the inversion of the resistivity data yielded information for the determination of the failure surface and presence of a fault in the Söke landslide area. According to ERT result in Line-3, it is in rotational form, and the depth to failure surface varies between 5 and 15 m. The borehole results also confirmed the presence of a fault in the site. In addition, the water-saturated zones indicated by low resistivities were identified. Moreover, the ERT was successful in detection of the consolidated and unconsolidated geologic units, which might have potential for future landslides. Comparison of the drilling and ERT results showed that they were in good agreement. The borehole results also confirmed the presence of a fault in the site.

Acknowledgements The authors thank Prof. Dr. Reşat Ulusay from Hacettepe University, Department of Geology for his helpful contributions and comments on the manuscript. We also thank to Assoc. Prof. Dr. Ö. Feyzi Gürer from Kocaeli University, Department of Geology for providing the geological map of the Söke and Kuşadası districts. Also we thank Asst. Prof. Dr. Gürkan Özden from Dokuz Eylül University, Department of Civil Engineering for his co-operation during the Söke landslide project.

References

Batayneh AT, Al-Diabat AA (2002) Application of a two-dimensional electrical tomography technique for investigating landslides along the Amman-Dead Sea highway, Jordan. Environ Geol 42:399–403

Bichler A, Bobrowsky P, Best M, Douma M, Hunter J, Calvert T, Burns R (2004) Three-dimensional mapping of a landslide using a multi-geophysical approach: the Quesnel Forks landslide. Landslides 1:29–40

Bogoslovsky V, Ogilvy A (1977) Geophysical methods for the investigation of landslides. Geophysics 42:562–571

Caris JPT, Van Asch Th WJ (1991) Geophysical, geotechnical and hydrological investigations of a small landslide in the French Alps. Eng Geol 31:249–276

Coggon JH (1971) Electromagnetic and electrical modelling by the finite element method. Geophysics 36:132–155

Dey A, Morrison HF (1979) Resistivity modelling for arbitrarily shaped two-dimensional structures. Geophys Prospect 27:106–136

deGroot-Hedlin C, Constable S (1990) Occam's inversion to generate smooth, two-dimensional models from magnetotelluric data. Geophysics 55:1613–1624

Geotomo software (2005a) Res2dmod software, ver. 3.0, http://www.geoelectrical.com

Geotomo software (2005b) Res2dinv software, ver. 3.52, http://www.geoelectrical.com

Griffiths DH, Barker RD (1993) Two-dimensional resistivity imaging and modelling in areas of complex geology. J Appl Geophys 29:211–226

Gürer ÖF, Bozcu M, Yılmaz K, Yılmaz Y (2001) Neogene basin development around Söke-Kuşadası (western Anatolia) and its bearing on tectonic development of the Aegean region. Geodinamica Acta 14:57–69

Hack R (2000) Geophysics for slope stability. Surv Geophys 21:423–448

Havenith HB, Jongmans D, Abdrakhmatov K, Trefois P, Delvaux D, Torgoev IA (2000) Geophysical investigations of seismically induced surface effects: case study of a landslide in the Suusamyr valley, Kyrgyzstan. Surv Geophys 21:349–369

Konagai K, Numada M, Zaferiakos A, Johansson J, Sadr A, Katagiri T (2005) An example of landslide-inflicted damage to tunnel in the 2004 Mid-Niigata prefecture earthquake. Landslides 2:159–163

Lapenna V, Lorenzo P, Perrone A, Piscitelli S, Sdao F, Rizzo E (2003) High-resolution geoelectrical tomographies in the study of Giarrossa landslide (southern Italy). Bull Eng Geol Environ 62:259–268

Loke MH, Barker RD (1996) Rapid least-squares inversion of apparent resistivity pseudosections using a quasi-Newton method. Geophys Prospect 44:131–152

McKenzie DP (1972) Active tectonics of the Mediterranean region. Geophys J R Astron Soc 30:109–185

Sarıca N (2000) The Plio-Pleistocene age of Büyük Menderes and Gediz grabens and their tectonic significance on N-S extensional tectonics in West Anatolia: mammalian evidence from the continental deposits. Geol J 35:1–24

Sasaki Y (1992) Resolution of resistivity tomography inferred from numerical simulation. Geophys Prospect 40:453–463

Seyitoğlu G, Scott B (1992) The age of Büyük Menderes graben (west Turkey) and its tectonic implications. Geol Magaz 129:239–242

Suzuki K, Higashi S (2001) Groundwater flow after heavy rain in landslide-slope area from 2-D inversion of resistivity monitoring data. Geophysics 66:733–743

Tripp AC, Hohmann GW, Swift CMJr (1984) Two-dimensional resistivity inversion. Geophysics 49:1708–1717

USGS (2004) Landslide types and processes. U.S. Department of the interior, U.S. Geological Survey, Fact Sheet, pp 2004–3072 http://www.pubs.usgs.gov/fs/2004/3072/FS2004-3072.pdf

Yang CH, Liu HC, Lee CC (2004) Landslide investigation in the Li-Shan area using resistivity image profiling method. In: SEG 74th annual meeting, Denver, Colorado, 10–15 October 2004

Yılmaz Y, Genç SC, Gürer Z, Altunkaynak S, Bozcu M, Yılmaz K, Elmas A (1999) Ege denizi ve Ege bölgesinin jeolojisi ve evrimi: (In Turkish) In: Türkiye denizlerinin ve Yakın çevresinin Jeolojisi, Görür N (ed.). Tübitak: İstanbul, pp 210–336